Chemical Physics 94 (1985) 265–271
North-Holland, Amsterdam

TRANSIENT PROPERTIES OF TRIPLET BOTTLENECK HOLEBURNING IN AN OPTICALLY THICK SAMPLE

F.W. DEEG [1], Larry MADISON [2] and M.D. FAYER

Department of Chemistry, Stanford University, Stanford, California 94305, USA

Received 6 July 1984; in final form 4 October 1984

The transient behavior of the light intensity transmitted through an optically thick sample of pentacene in *p*-terphenyl at 1.5 K after the onset of cw-dye laser excitation of the S_0 to S_1 transition of the O_3-site is reported. S-shaped curves with unusually long response times are found. A population-kinetic approach is developed which calculates the effect of populating the triplet state on the time dependence of the transmitted light intensity. The numerical calculations based on the bottleneck holeburning mechanism show good agreement with the experimental data without recourse to adjustable parameters. It is shown that the determination of $T_1 \rightarrow S_1$ ISC-rates in the picosecond and nanosecond range is possible through an experiment on a microsecond timescale.

1. Introduction

During the late sixties the development of high-power lasers and new devices for *Q*-switching and mode-locking stimulated research in the field of saturable absorbers. The experimental data were analyzed and theoretical predictions were made on the basis of a population-kinetic approach. The most important features are the saturation intensity, I_s, a measure of the intensity level at which non-linear absorption effects are significant, and the temporal response of the saturable filter to an incoming pulse of light. As the pulses considered were short (≈ 10 ns) most studies [1,2] focused on two-level systems, neglecting branching to long-lived levels, for example, the lowest triplet state, T_1, in organic dyes. In most cases the dynamic response of an optically thick sample to an incident light pulse with high intensity and short duration was in good agreement with the experimental data. Other studies [3,4] took into account a third "slow" level and derived an analytical solution for the temporal response of an optically *thin* sample. More recently, density matrix formalism has been applied to the problem of optically thin samples [5]. Expressions for the steady-state transmission of an optically thick absorber have also been given [3,6]. The temporal response of an optically thick absorber with a three-level system has not previously been investigated experimentally or theoretically. It was assumed that this response could be approximated by the solution for the optically thin case, that is, the transmitted intensity is described by an exponential asymptotically approaching the steady-state value with a response time not longer than the lifetime of the "slow" third level. Many studies of this type considered only bleaching of homogeneously broadened transitions and not holeburning in inhomogeneously broadened lines. However, some treatments included inhomogeneous broadening [5].

We have investigated the saturation dynamics of an optically thick sample of the mixed crystal pentacene/para-terphenyl at 1.5 K after laser excitation of the S_0 to S_1 O_3 site origin at $\lambda = 585.8$ nm. This system shows two major differences from optically thick systems considered earlier. (1) At 1.5 K the homogeneous linewidth of pentacene/

[1] Permanent address: Institut für Physikalische Chemie, Universität München, Sophienstrasse 11, 8000 Munich 2, FRG.
[2] Permanent address: Lawrence Livermore Laboratory, Livermore, California, USA.

p-terphenyl is 3–4 orders of magnitude smaller than the inhomogeneous broadening. That is saturation means holeburning and not bleaching. (2) The fact that the triplet state, T_1 acts as a bottleneck in which the excited molecules are caught implies that the saturation intensity is very low, namely 10 W/m^2 compared to 10^4–10^7 W/m^2 in the systems considered earlier. This low saturation intensity allows us to perform high OD saturation experiments with a cw laser. For the first time we can observe the saturation of a three-level system in an optically thick sample on the timescale of the "slow" level. Recording the time dependence of the transmitted intensity we find that the shape as well as the response time of the curves are distinctly different from results on optically thin absorbers. A numerical analysis based on a population-kinetic approach presented below explains the new features by the effects of the time dependence of the spatially-dependent light intensity on the holeburning.

Qualitatively, the difference between triplet bottleneck holeburning in optically thin and optically thick samples can be viewed as follows. In an optically thin sample the front, middle and back of the sample experience the same light intensity since, by definition, there is negligible absorption in an optically thin sample. Thus when a laser field of a particular intensity is turned on, the populations of the states in all parts of the sample evolve in the same manner, and this evolution is controlled only by molecular parameters, e.g., the triplet lifetime. However, in an optically thick sample with an OD of 3 or 4, when the laser field is turned on, the front of the sample experiences an intensity which is 10^3 to 10^4 greater than the back of the sample. If we imagine the sample as composed of thin slices, at $t = 0$ the front slice will experience an intensity great enough to begin developing a significant hole while the back slice will not. The front slice will develop a hole on the timescale of the triplet lifetime. This causes the second slice to see a large field, and it begins to hole burn on the timescale of the triplet lifetime. As each successive slice develops a hole, the field rises at the back of the sample. The net result is that the laser beam must dig a tunnel through the sample by holeburning each slice. When the tunnel reaches the back of the crystal, the high OD holeburning process is complete. Thus, the time dependence of the tunnel formation and therefore the time dependence of the light intensity emerging from the back side of the sample, depends both on molecular properties and the macroscopic properties of the sample.

As the laser digs through the sample, the tunnel increases its spread in frequency as well. The light field is large at the front of the crystal. There is substantial power-broadening producing a spectrally wide hole. At the back of the crystal, the field at $t = 0$ is weak and there is little or no power broadening. As slices of the sample near the front develop deep holes, the field rises at the back, increasing the hole depth and (because of increased power broadening) the hole width. Thus there is a complex time development of both the hole depth and frequency spread.

2. Experimental procedures

The pentacene/*p*-terphenyl crystals were grown from the melt by the Bridgman technique using extensively zone-refined *p*-terphenyl. The pentacene, obtained from Aldrich, was used without further purification. The crystals were cleaved along the *ab*-plane. The optical axis was located with an conoscopic microscope and the samples were mounted on 200 μ pinholes with the crystal *b*-axis parallel to the polarization direction of the exciting laser.

The laser used for holeburning was a Coherent model 599-21 single-mode scanning cw dye laser pumped by the 514 nm line of a Coherent Innova 90 argon ion laser. Single mode operation was monitored by a Tropel 240 spectrum analyzer. Maximum dye-laser power was 40 mW with 3 MHz bandwidth. The size of the laser beam was 200 μ in all experiments. The excitation wavelength was in the range 585.7–585.8 nm. The laser light was switched on and off by a Pockels cell with 1 ns risetime. The light transmitted through the crystal was monitored by a 1P28 PMT and recorded by a computer-interfaced R7912 Tektronix transient digitizer. Pockels cell and digitizer were triggered by the same signal from a

frequency generator. The OD and the lineshape of the O_3-site of the electronic origin of pentacene/*p*-terphenyl were measured with a 150 W high pressure Xe lamp and a 1 m SPEX scanning monochromator. To obtain the OD, the transmission through a 200 μ pinhole and sample was compared to the transmission through an identical pinhole without sample. Considerable care was taken to assure that only light passing through the pinholes reached the phototube. The error in the OD is estimated to be less than 0.1. The results shown in this paper were obtained from a crystal with a maximum OD of 3.7 and an inhomogeneous linewidth of 55 GHz. Equivalent results were obtained from a wide variety of other samples. The sample was immersed in liquid helium in a glass dewar that was pumped below the λ-point.

3. Results and discussion

Fig. 1 displays the intensity of light as a function of time transmitted by a sample of pentacene/*p*-terphenyl at 1.5 K after the onset of laser excitation of the O_3-site origin at 585.8 nm. The transients shown are for three optical densities (ODs), fig. 1a, and three different laser light intensities incident on the sample, fig. 1b. OD in this text always means small-signal-OD as seen by a sufficiently low-intensity light source. The OD was varied by tuning the laser to different places in the inhomogeneous line. To more clearly illustrate the temporal response of the system, the abscissa shows the transmitted intensity $I(t)$ divided by the steady-state transmitted intensity $I(t \rightarrow \infty)$. The absolute values of $I(t \rightarrow \infty)$ are given in the figure caption for each curve. The solid curves through the data are calculated using the procedure described below.

There are two significant features in fig. 1. (1) S-shaped transients are observed in contrast to the purely exponential behavior of an optically thin three-level system [3–5]. (2) Response times longer than the lifetime of the slow third level (45 μs in pentacene/*p*-terphenyl [7]) especially for high ODs and low incident light levels are observed.

To analyze the results presented in figs. 1a and 1b, we have chosen a simple energy-level diagram as shown in fig. 2. Levels $|1\rangle$ and $|2\rangle$ denote the ground and first excited singlet state, level $|3\rangle$ the first excited triplet state, the k_{ij} are the decay rate constants of these levels, and w is the absorption

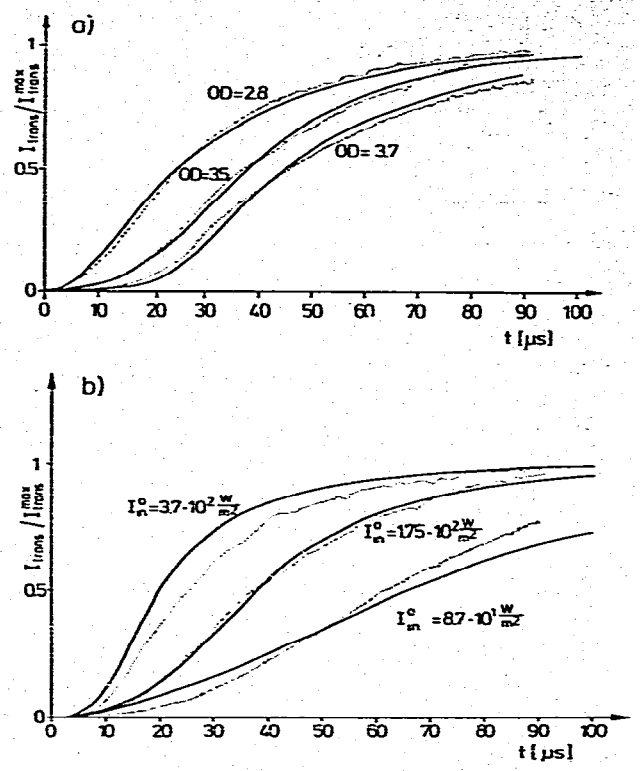

Fig. 1. (a) Transmitted intensity through a sample of pentacene/*p*-terphenyl after the onset of laser excitation of the O_3-site at 1.5 K for various optical densities (ODs). The dotted lines represent the experimental data, the solid lines are the results of the calculations described in the text. All data are for an incident intensity $I_{in}^0 = 1.75 \times 10^2$ W/m^2. To clearly illustrate the temporal behavior of different ODs, the transmitted intensity is divided by the maximum transmitted intensity occurring at $t = \infty$, which is different for each OD. The ODs given in the figure are the low light intensity (no holeburning) ODs. The actual maximum transmissions for the three curves are (top to bottom) 33%, 21%, and 19%. (b) Transmitted intensity through a sample of pentacene/*p*-terphenyl after the onset of laser excitation in the O_3-site at 1.5 K for various light intensities. The dotted lines represent the experimental data, the solid lines are the results of the calculations described in the text. All data are for a sample OD = 3.5. The maximum transmissions for the three curves are (top to bottom) 45%, 21% and 6%.

as shown in fig. 2. Levels $|1\rangle$ and $|2\rangle$ denote the ground and first excited singlet state, level $|3\rangle$ the first excited triplet state, the k_{ij} are the decay rate constants of these levels, and w is the absorption

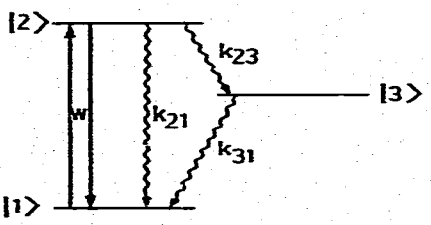

Fig. 2. Energy-level diagram and transitions used in the theoretical model.

and induced emission rate. We have used a pure population-kinetic approach and not a more general set of coupled Maxwell and optical Bloch equations. This is justified as the timescale of the experiments is much longer than T_2 ($T_2 = 19$ ns [8]).

We start with the following set of equations:

$$N_1 + N_2 + N_3 = N_0, \tag{1a}$$

$$dN_2/dt = -(k_{21} + k_{23})N_2 + w(N_1 - N_2), \tag{1b}$$

$$dN_3/dt = k_{23}N_2 - k_{31}N_3, \tag{1c}$$

$$dI/dx = -\alpha_0 I(N_1 - N_2)/N_0. \tag{2}$$

Here N_i are the population numbers, N_0 the total number of molecules, I the light intensity and α_0 the small-signal absorption coefficient. To couple eqs. (1) and (2) we need a relation between the pump rate w and the light intensity I. For the interaction of a perfectly monochromatic radiation field with the angular frequency ω and an infinitely sharp molecular transition with the angular frequency ω_0 the pump rate for $t \to \infty$ is given by [8,9]

$$w_{t\to\infty} = (\pi/2\hbar^2)|\hat{E}_0 \cdot \hat{\mu}|^2 \delta(\omega - \omega_0). \tag{3}$$

Here $\hat{E}_0$ denotes the electric field vector and μ the transition dipole moment. We can neglect the very small linewidth of the laser light in our case but we have to take care of the homogeneous linewidth of the molecular transition by convoluting eq. (3) with a lorentzian lineshape function

$$\frac{1}{\pi T_2}\frac{1}{(\omega-\omega_0)^2 + (1/T_2)^2}, \tag{4}$$

which gives us

$$w_{t\to\infty} = \frac{T_2}{2}\left(\frac{\hat{\mu}\cdot\hat{E}_0}{\hbar}\right)^2 \frac{1}{T_2^2(\omega-\bar{\omega}_0)^2 + 1}. \tag{5}$$

T_2 is the transverse relaxation time and $\bar{\omega}_0$ the homogeneous line center. The introduction of the lorentzian lineshape function and the long time limit imposed on eq. (3) make eq. (5) valid only for times $t \gg T_2$. Eq. (5) describes the off-resonance pumping: molecules can be excited in the wings of the homogeneous line ($\omega \neq \bar{\omega}_0$) [7]. The relation between the external electric field in front of the sample and the light intensity is given by

$$E_{ext}^2 = 2I/v_{He}\epsilon_{He}, \tag{6}$$

where v_{He} and ϵ_{He} are the velocity of light and the permittivity of liquid helium at 1.5 K. Local-field corrections relating the electric field along the b-axis in the crystal and the external electric field have been calculated [10]. Using further the fact that the $S_1 \leftarrow S_0$ transition dipole moment of pentacene is along the short axis of the molecule and there is an angle of 34° between this axis and the crystal b-axis, we find the following numerical relation between the local electric field component parallel to the $S_1 \leftarrow S_0$ transition dipole moment and the intensity of light polarized along the crystal b-axis: $E_{loc}^2 = aI$ with $a = 1.6510\ v^2/W$.

Introducing this into eq. (5) and replacing $\omega - \bar{\omega}_0$ by $\Delta\omega$ we obtain

$$w = (T_2/2)(\mu^2 aI/\hbar^2) \times \left(\Delta\omega^2 T_2^2 + 1 + \tfrac{1}{2}aI\mu^2 T_2^2/\hbar^2\right)^{-1}. \tag{7}$$

The last term in eq. (7) takes into account power broadening effects at high laser intensities. In principle we still have to convolute this formula with the inhomogeneous lineshape, but the bandwidth of the molecules which are pumped is much smaller than the inhomogeneous linewidth even at the highest intensities used. Therefore we can neglect the finite inhomogeneous linewidth.

The important point in eq. (7) is the following: we have to deal with an optically thick sample, so the light intensity I is a function $I(x)$, where x is the distance into the absorbing sample. As the pump rate w not only explicitly depends on frequency but also on the intensity I we have to describe w as a function, $w(x, \Delta\omega)$, of frequency and distance. Since the populations, N_i, in eq. (1) depend on w, N_i are also functions of x and $\Delta\omega$.

Time is a third parameter, so that we finally obtain the following equations:

$$N_1(x, t, \Delta\omega) + N_2(x, t, \Delta\omega) + N_3(x, t, \Delta\omega) = N_0(\Delta\omega), \quad (8a)$$

$$dN_2(x, t, \Delta\omega)/dt = -(k_{21} + k_{23})N_2(x, t, \Delta\omega) + w(\Delta\omega, I(x, t))(N_1 - N_2)(x, t, \Delta\omega), \quad (8b)$$

$$dN_3(x, t, \Delta\omega)/dt = k_{23}N_2(x, t, \Delta\omega) - k_{31}N_3(x, t, \Delta\omega), \quad (8c)$$

$$dI(x, t)/dt = -I(x, t)(\alpha_0 T_2/N_0\pi) \times \int_{-\infty}^{+\infty} (N_1 - N_2)(x, t, \Delta\omega) \times \frac{1}{1 + \Delta\omega^2 T_2^2} d\Delta\omega. \quad (8d)$$

The integral in eq. (8d) calculates the absorption coefficient $\alpha(x, t)$ as seen by the light beam by convoluting the population difference $(N_1 - N_2)(\Delta\omega)$ with the homogeneous lineshape.

The numerical integration follows essentially the procedure described by Olson et al. [11]. The set of coupled partial differential equations are integrated over a three-dimensional grid with the axis $\Delta\omega$, x and t. The following Adams–Moulton predictor–corrector pair is used [11,12]. If $dy/dx = f(x, y)$ then

$$y_n^P = y_{n-1} + (h/2)(3f_{n-1} - f_{n-2}), \quad (9a)$$

$$y_n^C = y_{n-1} + (h/2)(f_n - f_{n-1}), \quad (9b)$$

where h is the step size. We cover the grid by taking a step along t, traversing x for this t-value, then taking another step along t, traversing x again, and so on. In traversing x, we calculate the populations N_i for every frequency component $\Delta\omega$, and then obtain $I(x)$ by performing the integration in eq. (8d). The program calculates the light intensity leaving the crystal at time t for a given incident intensity I_{in}^0 ($I_{in} = 0$ for $t < 0$, $I_{in} = I_{in}^0$ for $t > 0$) and a given OD of the sample. The molecular parameters used in the program are known from earlier experiments: $T_2 = 19$ ns [8], $k_{21} = 4.2 \times 10^7$ s^{-1}, $k_{23} = 7.5 \times 10^7$ s^{-1} [8], $\mu = 0.71$ D [7,13]. For the triplet relaxation rate k_{31} we used the value obtained by de Vries and Wiersma [7] in their fluorescence transient fits: $k_{31} = 2.2 \times 10^4$ s^{-1}. The results of the numerical integration based on these parameters are shown by the solid lines in figs. 1a and 1b. The values used for incident-light intensity and sample OD are those measured in the experiment.

Comparing the theoretical data with the experimental data we realize that the theory reflects all the essential features of the experiment without adjustable parameters and in fact gives reasonable quantitative agreement. We find S-shaped curves with response times longer than the triplet lifetime. The response time increases with increasing OD of the sample (fig. 1a) and with decreasing input intensity (fig. 1b). The quantitative agreement is very satisfactory in light of the approximations inherent in theory and experiment: (1) The experiment was performed with a laser beam waist of 200 μm through a pinhole with 200 μm diameter. The intensity distribution over the beam which traverses the sample is not uniform. At the center we have higher intensity and at the edge lower intensity than the average one assumed in the numerical integration. This problem can in principle be accounted for by performing the appropriate average [14]. However, the problem is compounded by crystal striations and cracks which significantly distort the intensity distribution. (2) Our model is based on a three-level system (see fig. 2). To obtain a correct picture of the molecular processes at 1.5 K we have to take into account the selective population and depopulation rates of the triplet sublevels [15]. Unfortunately there are no reliable data for these rates in the pentacene/*p*-terphenyl system so we cannot treat the full five-level system.

To illuminate the saturation dynamics in optically thick systems we have plotted in fig. 3 an intensity transient together with the time dependence of the absorption coefficient at the front and at the back of the sample. The graphs show that the light burns a deep hole into the absorption band of the first few layers of the sample very quickly. At short time there is essentially no saturation effect in the rear part of the sample; the light is too weak to induce any significant non-lin-

ear effects. As time goes on more and more light reaches deeper layers and finally the back of the crystal. The intensity transient reflects the pumping of molecules into the triplet bottleneck, one layer after the other. In the calculation of fig. 3, the low light level OD is 3.5, or 0.03% transmission. This is also the $t = 0$ transmission. The transmission at 100 μs is ≈ 7%. This corresponds to an increase in transmission of ≈ 250. In the long time limit, the transmission reaches ≈ 21%. Thus there is a slow time-dependent increase in the transmission of ≈ 700.

In the experiments described here, all the necessary molecular parameters are known, so the experiments can be compared to calculations without adjustable parameters. Curves such as those displayed in fig. 1 confirm the basic validity of the microscopic model embodied in eq. (8). In principle, a determination of $T_1 \leftarrow S_1$ ISC rates in the picosecond and nanosecond range is possible through this type of experiment on a microsecond timescale. This is illustrated in fig. 4. The solid and the dashed lines are two calculations of the experimental data. The only difference is that the solid line uses a quantum yield of 64% as given by the stimulated photon echo experiments of Patterson et al. [8] whereas the dashed line assumes a quantum yield of 36%. We see that the solid line provides a good fit while the dashed line falls well off the experimental data. Thus, if all other molecular parameters are known it is possible to determine the ISC rate constant. The experiment can be performed by a recording apparatus with low resolution in time (μs) and even by a broad-band laser if the calculation is extended to take into account the finite linewidth of the light source. De Vries and Wiersma [7] have shown how to determine triplet ISC-rates from fluorescence transients in optically thin samples. Their method is very sensitive for the evaluation of low triplet quantum yields. It becomes difficult to handle in the case of high quantum yields. Our method is useful for high quantum yields where the triplet bottleneck effect is large. For low quantum yields the absolute value as well as the change of the transmitted intensity are small because the holes burnt in the optically thick sample are shallow. This is demonstrated by the fact that for light intensities and ODs as shown in fig. 1 we could not detect any intensity transient if we tuned the laser to the G_1-site where other experiments revealed an ISC-yield < 0.5% [7,8].

Holeburning experiments in the laboratory have to deal with samples of a finite optical density. It is well-known that if this OD becomes consider-

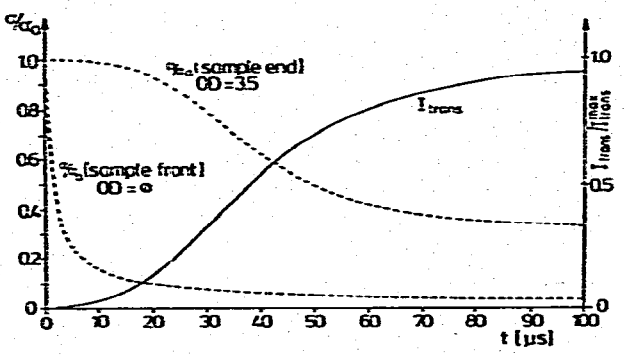

Fig. 3. Transient transmitted intensity (solid line) and concomitant change of the absorption at the front and at the back of the sample (dashed lines) for an OD = 3.5 and an incident light intensity $I_{in}^0 = 1.75 \times 10^{-2}$ W/m². α/α_0 denotes the ratio of effective absorption coefficient α and the low light level (no holeburning) absorption coefficient, α_0. The sample transmission climbs from 0.03% at $t = 0$ to ≈ 7% at 100 μs and will reach 21% in the long time limit. The α/α_0 curve for the front of the sample behaves as that of an optically thin sample. This is in marked contrast to the α/α_0 curve for the sample back.

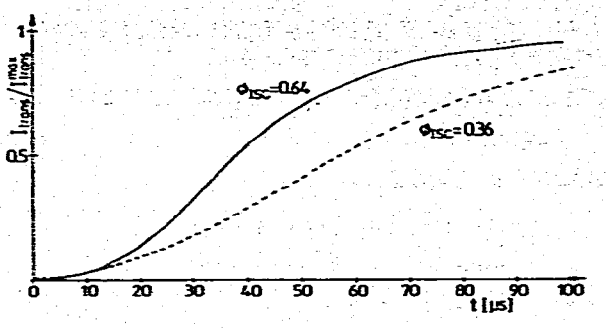

Fig. 4. Influence of triplet T_1 ISC-yield on intensity transients. The dotted line is the experimental graph for an incident light intensity $I_{in}^0 = 1.75 \times 10^{-2}$ W/m² and an OD = 3.5. The solid and the dased line represent the numerical calculations assuming a T_1 quantum yield of 64% or 36%. The other necessary molecular parameters are given in the text.

able, the hole size is different at the front and back of the sample. However, looking at the $\alpha(t)$ graphs in fig. 3 shows us that not only is the size of the holes different but so is the burning time to reach the maximum depth and frequency width. The use of holeburning for both fundamental research and practical applications is increasing. The results presented here provide a complete description of the transient properties of three-level holeburning in optically thick samples and give insight into the holeburning phenomenon in any finite OD sample.

Acknowledgement

The authors would like to thank H.W.H. Lee for many useful discussions concerning the numerical calculation. FWD would like to thank the DAAD for a short-term grant at Stanford. This work was supported by the National Science Foundation, Division of Materials Research (#DMR79-20380). MDF would like to thank the Guggenheim Foundation for a fellowship which contributed to this work.

References

[1] F. Gires and F. Combaud, J. Phys. (Paris) 26 (1965) 325.
[2] A.C. Selden, Brit. J. Appl. Phys. 18 (1967) 743.
[3] M. Hercher, Appl. Opt. 6 (1967) 947.
[4] B. di Bartolo, Optical interactions in solids (Wiley, New York, 1968) pp. 431–442.
[5] H. de Vries and D.A. Wiersma, J. Chem. Phys. 72 (1980) 1851;
W.E. Moerner, A.R. Chraplyvy and A.J. Sievers, Phys. Rev. B29 (1984) 6694;
M. Romagnoli, W.E. Moerner, F.M. Schellenberg, M.D. Levenson and G.C. Bjorklund, J. Opt. Soc. Am. B1 (1984) 341.
[6] R.W. Keyes, IBM J. 7 (1963) 334.
[7] H. de Vries and D.A. Wiersma, J. Chem. Phys. 70 (1979) 5807.
[8] F.G. Patterson, H.W.H. Lee, W.L. Wilson and M.D. Fayer, Chem. Phys. 84 (1984) 51, and references therein.
[9] W.H. Louisell, Quantum statistical properties of radiation (Wiley, New York, 1973) ch. 5.
[10] J.H. Meyling, P.J. Bounds and R.W. Munn, Chem. Phys. Letters 51 (1977) 234.
[11] R.W. Olson, H.W.H. Lee, F.G. Patterson and M.D. Fayer, J. Chem. Phys. 76 (1982) 31.
[12] G. Dahlquist and A. Bjoerk, Numerical methods (Prentice-Hall, Englewood Cliffs, 1974).
[13] H. de Vries and D.A. Wiersma, J. Chem. Phys. 69 (1978) 897.
[14] P. Kolodner, J.G. Black and E. Yablonovitch, Opt. Letters 4 (1979) 38.
[15] M.F.A. El-Sayed, Ann. Rev. Phys. Chem. 26 (1975) 235.